Chapter 5

Amphiphilic counterion activators for DNA[§]

5.1 Introduction[§]

Cell-penetrating peptides (CPPs)[1] are guanidinium-rich oligomers and polymers that have attracted much attention because of their biological importance to help cellular uptake of various molecular cargos on the one hand and their complex behaviour on the other. It was suggested early on that the activities of weakly acidic polycations in general are determined by their need to strongly bind multiple counteranions in order to minimize intramolecular charge repulsion.[2,3] Building on this concept of counterion-mediated function, balanced combinations of amphiphilic and hydrophilic counteranions were found to enable oligo- and polyarginines to dissolve in chloroform,[2] partition from water into chloroform,[2] move across bulk and lipid bilayer membranes,[2] and enter into living cells,[4] (see also the **Introduction** to **Chapter 4**). Other expressions of the same concept were shown to account for the voltage gating of biological potassium channels[5] and the conductance and selectivity of synthetic ion channels.[6] Moreover, CPP-counteranion complexes were also found to transport anions across bulk and bilayer membranes,[2] a property that was exploited in the development of stimulus-responsive CPP-counteranion complexes as multi-enzyme detectors[7] and multi-analyte sensors.[8]

The rich multifunctionality that results from counteranion activation of polycations such as CPPs raised the possibility that the charges could be inverted,[3] i.e., that a countercation could form a complex with an anion, such as DNA, and achieve the same function. The cellular uptake of countercation-activated DNA and other weakly basic polyanions mirrors perfectly the cellular uptake of counteranion-activated CPPs and other weakly acidic polycations; the only difference is that the latter process can be spontaneous due to the presence of anionic phospholipid activators in biological membranes. It was wondered whether a DNA-countercation complex could be developed that rivals the multifunctionality of CPPs, such that DNA molecules could be activated to function as cation transporters, multi-enzyme detectors, or multi-analyte sensors.[3]

In the work reported in this chapter calf thymus DNA was found to be successfully activated by amphiphilic cations and it could transport cations across bulk and lipid bilayer membranes.

[§]In this chapter many compounds and procedures are indicated in abbreviated forms. To help the reader, a summary of these abbreviations are reported in the following legend

CPP: cell-penetrating peptides; ctDNA: Calf thymus DNA; DG: dodecylguanidinium; DPX: p-xylene-bis-pyridinium bromide; CF: 5(6)-carboxyfluorescein; HPTS: 8-hydroxy-1,3,6-pyrenetrisulfonate; EYPC-LUVs⊃DPX/HPTS: egg yolk phosphatidylcholine large unilamellar vesicles loaded with the anionic fluorophore HPTS and the cationic quencher DPX; pK: poly-L-lysine.

The ion-carrier properties of counterion-activated DNA were first characterized using the "U-tube" technique[2,9] and in vesicles. Subsequently, a series of amphiphilic, bola-amphiphilic, aliphatic, aromatic, and macrocyclic ammonium and guanidinium countercations was used, to ascertain the nature of DNA activation. Finally, using phytase and phytate as examples, the unusual activity of DNA was explored in the context of multi-analyte sensors.[10,11]

5.2 Results and Discussion

5.2.1 DNA-Countercation Complexes as Cation Carriers in Bulk Membranes[◊]

To investigate the properties of our compounds, at the beginning, U-tube experiments were performed, because, in contrast to the more complex lipid bilayer membranes, they provide straightforward and unambiguous evidence for existence and selectivity of ion carriers.[2a,9] In a typical experiment, a hydrophobic chloroform phase, or "bulk membrane", was placed at the bottom of the U-tube and covered on both the cis and the trans side of the wall with separate aqueous phases (**Fig. 5.1D**). Calf thymus DNA (ctDNA) was employed as a representative carrier, and dodecylguanidinium (DG) was used as a representative amphiphilic counterion activator. ctDNA and/or DG were added to the cis buffer together with a hydrophilic reporter ion;[2a] the concentration of this reporter ion in the trans buffer was monitored as a function of time (**Fig. 5.1**). Safranin O[12,13] was selected initially as a convenient reporter cation (**Fig. 5.1**). Only in the presence of ctDNA-DG complex safranin O moved efficiently from the cis aqueous phase across the bulk membrane to the trans aqueous phase (**Fig. 5.1A**, ●); no transport was observed in the absence of the complex (**Fig. 5.1A**, ○). Neither ctDNA (**Fig. 5.1A**, □) nor DG activator alone (**Fig. 5.1A**, X) was able to transport safranin O with comparable efficiency in the U-tube.

[◊]*All transport experiments here reported were carried out by Toshihide Takeuchi, in the laboratory of Prof. Stefan Matile at the University of Geneva. The synthesis of the calix[n]arenes and of the Gemini compounds was performed in our laboratory in Parma, while the synthesis of alkyl and aryl ammonium, and alkyl guanidinium compounds was performed by Toshihide Takeuchi.*

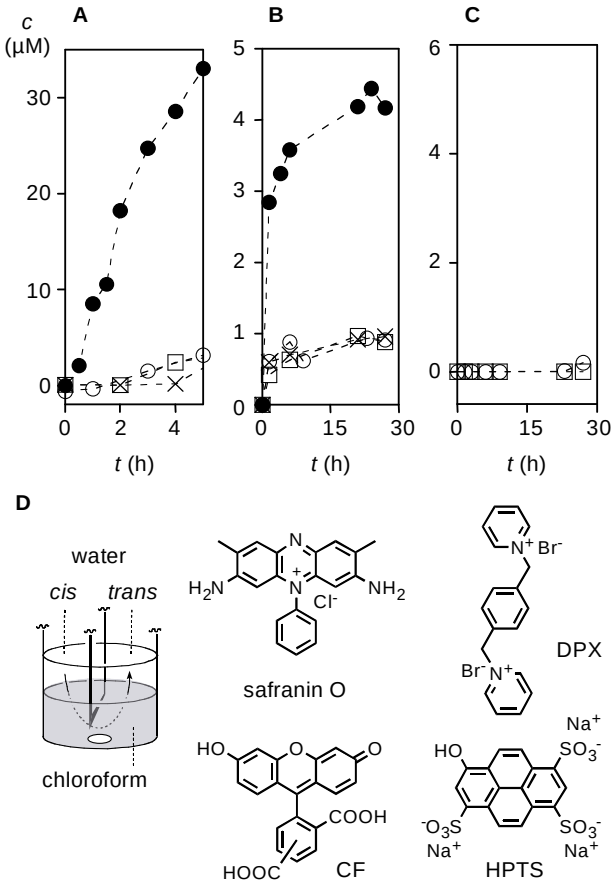

Fig. 5.1. DNA-counterion complexes as cation carriers in the U-tube. (**A**) safranin O (100 μM) transferred from cis buffer (0.5 mL) across bulk chloroform membranes (3 mL) into trans buffer (0.5 mL) as a function of time in the presence of calf thymus DNA (●, □; 1.25 μg/mL cis) and DG (●, X; 50 μM cis). Buffer: 10 mM Tris, 107 mM NaCl, pH 7.4. (**B**) Same for DPX (100 μM cis) with ctDNA (●, □; 1.25 μg/mL cis) and DG (●, X; 50 μM cis). (**C**) Same for CF (○, 100 μM cis) and HPTS (□, 100 μM cis) with ctDNA (○, □; 1.25 μg/mL cis) and DG (○, □; 50 μM cis). (**D**) Experimental setup for U-tube experiments, and structure of cationic and anionic probes used. The term "U-tube experiment" is maintained although modern versions of U-tubes are often not U-shaped.

The ability of DNA-counterion complexes to transport p-xylene-bis-pyridinium bromide (DPX)[12,13] across bulk chloroform membranes was studied next. Changes in the RP-HPLC profiles of the trans phase over time suggested that ctDNA-DG complexes were acting as carriers of DPX in bulk membranes (**Fig. 5.1B**, ●). Control experiments confirmed that DPX is not transported without the presence of the DNA-counterion complex (**Fig. 5.1B**, (○, □, X)). The observed transport of aromatic cations such as DPX and safranin O by ctDNA-DG carriers is potentially interesting because binding to DNA duplexes could occur not only by competitive counterion exchange at the polyphosphate backbone but possibly also by non-competitive intercalation into the π-stack. However, it was previously shown that counterion-activated polyions other than double-stranded DNA are able to transport DPX. This

observation does not support the hypothesis of that intercalation contributes significantly to transport.[3]

The ability of DNA-countercation complexes to carry anions across bulk chloroform membranes was evaluated with 5(6)-carboxyfluorescein (CF)[12,13] and 8-hydroxy-1,3,6-pyrenetrisulfonate (HPTS) as classical reporter anions. No anion transport activity was observed under conditions where ctDNA-DG complexes functioned as efficient cation carriers (**Fig. 5.1C**). Taken together, these U-tube experiments provided compelling experimental evidence that DNA-counteranion complexes can function as selective cation carriers.

5.2.2 DNA-Countercation Complexes as Transporters in Lipid Bilayer Membranes

The ability of DG-activated ctDNA to act as a cation transporter in lipid bilayer membranes was determined in EYPC-LUVs⊃DPX/HPTS (i.e., egg yolk phosphatidylcholine large unilamellar vesicles loaded with the anionic fluorophore HPTS and the cationic quencher DPX).[2c] Under these conditions, cation export (DPX), anion export (HPTS), and vesicle lysis are all reported as an increase in fluorescence emission of DPX (**Fig. 5.2**). According to the HPTS/DPX assay, ctDNA and DG alone were inactive. Together, however, they were active (**Fig. 5.2**). The fluorescence recovery in response to the addition of ctDNA-DG complexes was calibrated against vesicle lysis and reported as fractional activity *Y*. Dose response curves for *Y* against the concentration of either the countercation activator or the DNA transporter gave the corresponding EC_{50}'s, the effective concentration needed to reach $Y_{MAX/2}$ (**Fig. 5.2B** and **Experimental**). The uptake of carriers into intact vesicles can be difficult to detect unambiguosly.[2c,14] However, because DNA-counterion complexes have been shown to enter cells[15,16] and to move across bulk chloroform membranes (**Fig. 5.1**), it was hypothesized that DNA uptake into vesicles was likely possible. To confirm this hypothesis, using the same conditions as above, EYPC-LUVs⊃DPX/HPTS were loaded with increasing concentrations of poly-L-lysine (pK). As a result, an increase in the EC_{50} and a decrease in Y_{MAX} of the ctDNA-DG transporters were observed (**Fig. 5.2B** and **Table 5.1**). This inactivation of extravesicularly added DNA by intravesicular pK could be interpreted to result from inactivation of DNA uptake by binding to the hydrophilic polycation in the vesicles. Decreasing Y_{MAX} and increasing EC_{50} in the dose response curves for DNA suggested that an

inactive pK-ctDNA-DG complex was formed within the vesicles that prevented transport of DNA, and therefore DPX, across the lipid bilayer.

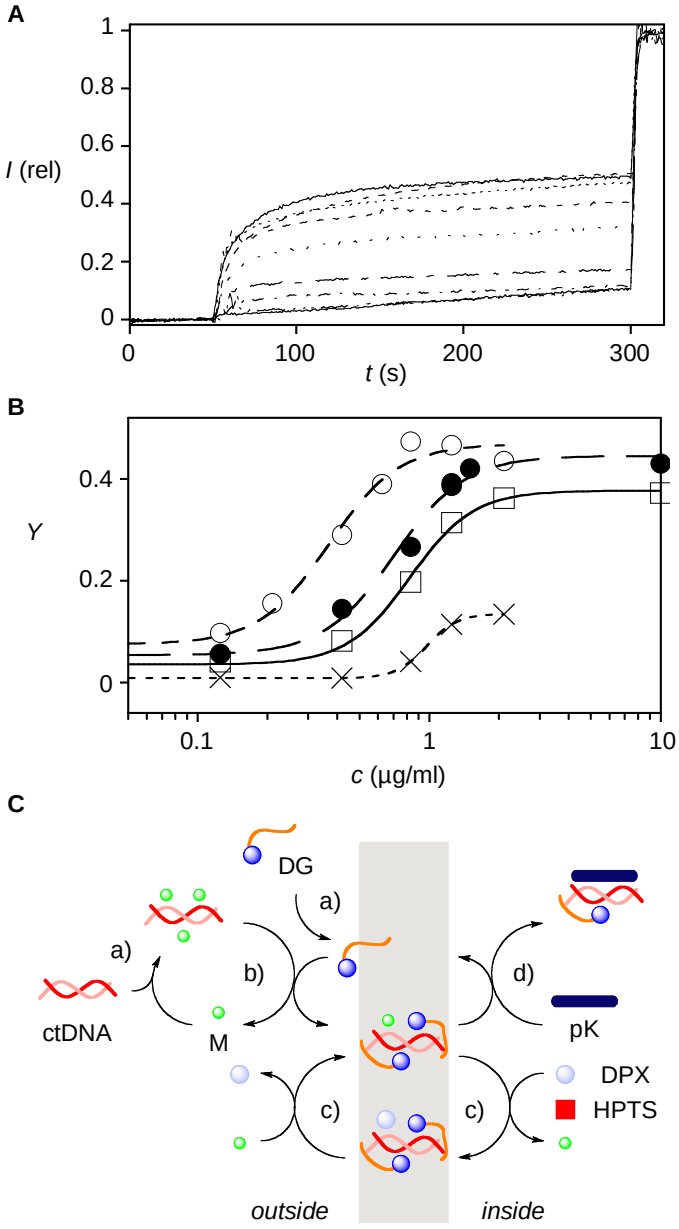

Fig. 5.2. Dependence of the activity of DNA-counterion complexes on the concentration of DNA (A, B) and internal counterion inactivators (B). (**A**) Fractional HPTS emission I (λ_{ex} 413 nm, λ_{em} 511 nm) as a function of time during the addition of calf thymus DNA (t = 50 s, (a) 0, (b) 0.2, (c) 0.3, (d) 0.5, (e) 0.7, (f) 1.0 and (g) 2.0 μg/ml final concentrations) to EYPC-LUVs⊃HPTS/DPX (~12.5 μM lipid) in the presence of external DG (50 μM). Conditions: 5 mM HPTS, 16.5 mM DPX, 10 mM Tris, 72 mM NaCl, pH 7.4 (inside); 10 mM Tris, 107 mM NaCl, pH 7.4 (outside), 25 ºC, calibrated by final addition of triton X-100, t = 300 s). (**B**) Dose response curves for DNA at constant concentration of external activator DG and increasing concentration of internal inactivator pK (0 (○), 1 (●), 10 (□) and 100 μM (×) inside; with curve fits to Hill equation, see **Table 5.1**). (C) Experimental setup for vesicle experiments: (**a**) Addition of polyions (e.g., ctDNA) and counterion activators (e.g., DG) to vesicles with internal reporter ions (e.g., DPX, HPTS) and counterion inactivators (e.g., pK) possibly causes (**b**) the formation of membrane-active polyion-counterion complexes (e.g., ctDNA-DG), (**c**) DPX export, (**d**) the formation of internal polyion-counterion complexes (e.g., ctDNA-DG-pK), etc; M = Na.

Table 5.1. Inactivation of ctDNA-DG transporters by intravesicular polylysine (pK).[a]

	Poly-L-lysine (μM)	EC_{50} (μg/mL)[b]	Y_{MAX} (%)[c]
1	0	0.37 ± 0.04	47 ± 2
2	1	0.71 ± 0.06	45 ± 2
3	10	0.83 ± 0.04	38 ± 1
4	100	0.98 ± 0.01	14 ± 0.1

[a]From DPX/HPTS export from EYPC-LUVs⊃DPX/HPTS at constant concentration of DG activators (50 μM), 10 mM Tris, 107 mM NaCl, pH 7.4, 25 ˚C, see **Fig. 5.2**. [b]Effective DNA concentration needed to reach 50% activity ($Y_{MAX/2}$), data ± SE. From Hill analysis of dose response curves in **Fig. 5.2**. [c]Maximal fractional fluorescence emission relative to lysis.

This interpretation, however, was not conclusive because the binding of DNA to intravesicular pK, extravesicular pK and freshly released pK should give exactly the same result. To detect uptake into intact vesicles more convincingly, sequential DNA addition to vesicles with internal pK inactivators and external DG activators was explored (**Fig. 5.3**). The total DNA concentration was selected to produce nearly complete fluorescence recovery when added all at once (**Fig. 5.3A** solid line, and **5.2B**). Addition of the same amount of DNA in several small portions produced essentially no activity (**Fig. 5.3A**, dashed line). Clearly, stepwise DNA addition was not additive. This non-additivity demonstrated that, at low concentrations, DNA-DG complexes move across bilayer membranes non-destructively and are trapped by pK within intact vesicles. pK release during counterion-mediated DNA uptake would make sequential DNA addition additive. Control experiments confirmed that sequential DNA addition to vesicles without intravesicular pK inactivators is additive (**Fig. 5.3B**).

The same additivity was found to occur with extravesicular rather than intravesicular pK inactivators (**Fig. 5.3C**). The resulting uniqueness of non-additive activity of DNA-counterion with intravesicular pK only confirmed that this phenomenon originates from non-destructive DNA uptake into and trapping within intact vesicles.

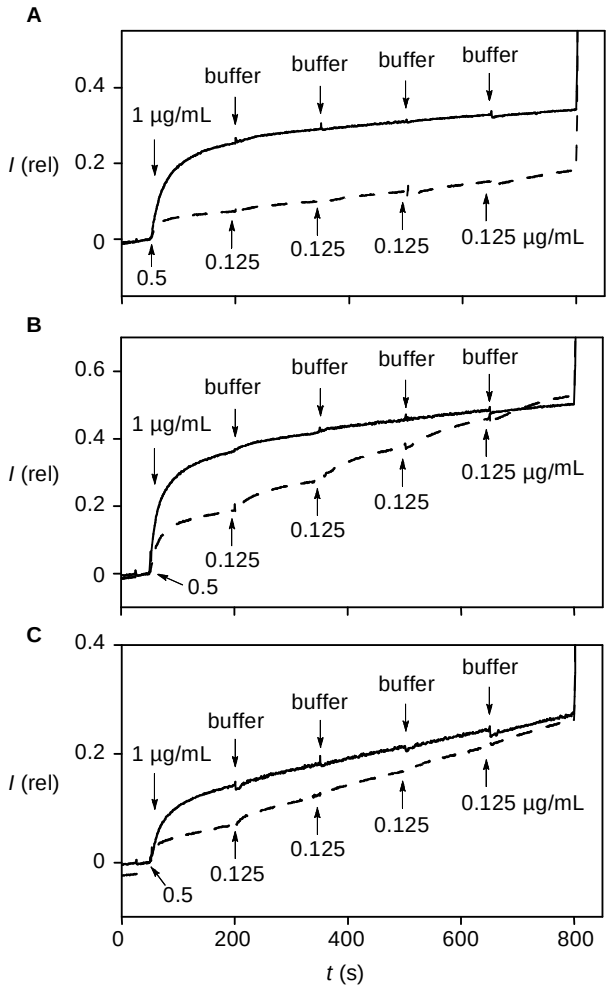

Fig. 5.3. Fractional HPTS emission I during the addition of ctDNA at t = 50 s (1.0 µg/mL final; solid traces) or at t = 50 s (0.5 µg/mL), t = 200 s (0.125 µg/mL), t = 350 s (0.125 µg/mL), t = 500 s (0.125 µg/mL) and t = 650 s (0.125 µg/mL; dashed traces) to EYPC-LUVs⊃HPTS/DPX (~12.5 µM lipid) with external DG (50 µM) and (A) with internal pK (10 µM), (B) without pK, or (C) with external pK (10 nM). Conditions as in **Fig. 5.2**.

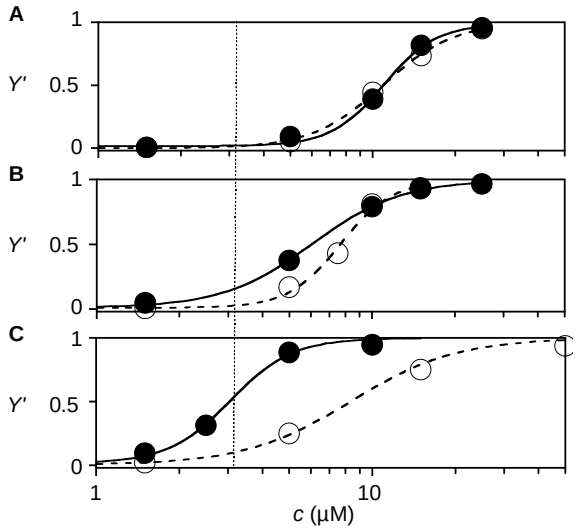

Fig. 5.4. Dose response curves for the activation of calf thymus DNA (12.5 µg/mL) by calix[4]arene **5a** (increasing concentrations) in EYPC-LUV⊃HPTS/DPX (●) and EYPC-LUV⊃CF (○) at (**A**) ~75 µM, (**B**) ~50 µM and (**C**) ~25 µM EYPC. Fractional activities *Y* from conventionally calibrated curves were normalized to maximal (*Y*' = 1 = Y_{MAX}) and minimal (*Y*' = 0) before lysis.

Different to the HPTS/DPX assay, the CF assay fails to detect cation export and reports on anion export and lysis only.[13] As representative examples of the synthesized cations, the activation of calf thymus DNA by DG **74**[3a] or calix[4]arene **5a** was nearly identical in EYPC-LUVs⊃HPTS/DPX and EYPC-LUVs⊃CF (**Fig. 5.4A** and **5.5**). As a response to vesicle dilution, the HPTS/DPX assay revealed decreasing EC50's, whereas constantly high EC50's were found in the CF assay (**Fig. 5.4A-C**). High EC50's with independence on vesicle concentration supported that the CF assay detects larger pores or more dramatic events that depend only on the CMC of higher-order DNA-counterion assemblies (**Fig. 5.4A-C**, ○). Low EC50's with dependence on vesicle concentration demonstrated that HPTS/DPX assay reports indeed on cation transporters (**Fig. 5.4A-C**, ●). The differences found between HPTS/DPX and CF assay thus suggested that under mild conditions, DNA-counterion complexes can act as cation transporters in intact vesicles (**Fig. 4C**, ● vs ○). In the present example, this is the case of **5a** around 3 μM, ctDNA 12.5 μg/ml, and EYPC ~25 μM (**Fig. 5.4**, dotted line). The validity of this interpretation was confirmed by U-tube and intravesicular trapping experiments (**Fig. 5.1** and **5.3**). The apparent transition from non-destructive cation transport toward the formation of larger pores and more dramatic events at higher concentrations of DNA-counterion complexes was not surprising. The concentration dependence of transport mechanisms, usually shifting from carriers over channels and pores toward detergents with increasing concentration, has been suggested from also prominent examples such valinomycin, melittin or triton X-100.[17]

The dependence of the activity of ctDNA-DG complexes on other variables was not a surprise. For instance, EC50's increased and Y_{MAX} decreased with increasing ionic strength (**Fig. 5.10**, see **Experimental**). This finding confirmed the importance of ion pairing and ion exchange for the activity of ctDNA-DG complexes. Low membrane fluidity gave poor efficiencies (**Fig. 5.11**, see **Experimental**). This trend was consistent with but not exclusive for an ion carrier mechanism.[2,13,18] The presence of anionic lipids in the bilayer did not much influence efficiencies (**Fig. 5.12**). This insensitivity of polyanionic DNA to anionic phospholipids was in meaningful contrast to the strong dependence of polycationic CPPs and potassium channels, where anionic lipids in the membrane can act as intrinsic counterion activators.[2,5]

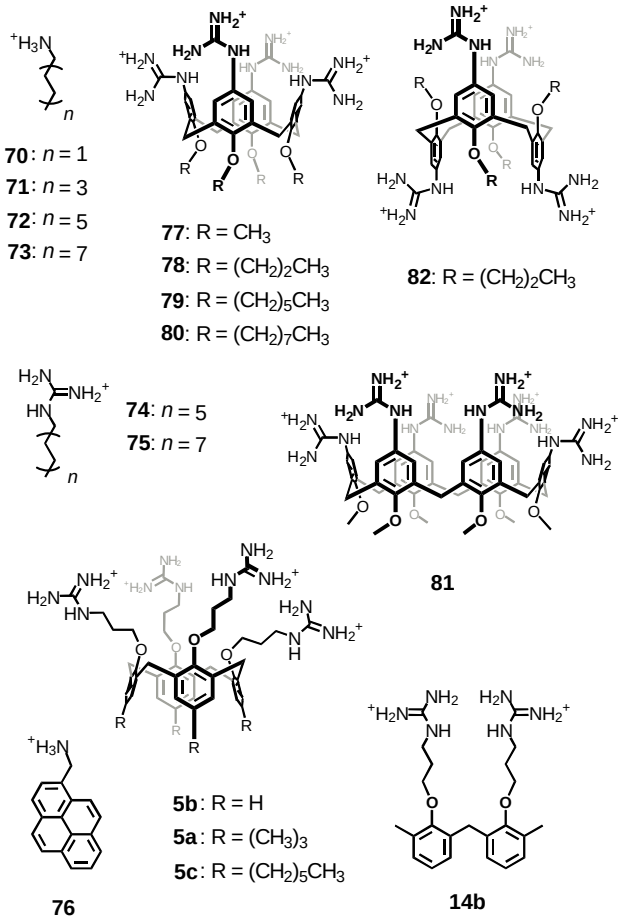

Fig. 5.5. Countercation activators for DNA carriers, detectors and sensors.

5.2.3 Counterion Activators

The activity of countercation-activated polyanions beyond DNA decreased with increasing basicity of the involved anions (DNA, RNA, polyphosphate >> hyaluronan, polyglutamate).[3] This series complemented the decreasing activity of counteranion-activated polycations with increasing acidity of the involved cation and thus confirmed intramolecular charge repulsion as general origin of counterion-mediated function.[2,3]

To quantify the activation of calf thymus DNA by all the amphiphiles, their EC_{50}'s, maximal activities Y_{MAX}, and efficiencies η[2b] were determined (**Fig. 5.13** in the **Experimental Section** and **Table 5.2**). The results revealed that high activator hydrophobicity is essential for high η. Ammonium cations (**70**-**73**) were less efficient than guanidinium cations (**74**, **75**). This trend was not further surprising considering the preference of phosphate anions to pair with guanidinium rather than ammonium cations.[2,19]

Table 5.2. Countercation activators of DNA transporters.[a]

	Activator	Charge[b]	EC_{50} (μM)[c]	Y_{MAX} (%)[d]	η[e]
1	**70**	+1	-	-	-
2	**71**	+1	-	-	-
3	**72**	+1	108 ± 5	100 ± 3	34
4	**73**	+1	7.7 ± 1.4	73 ± 5	57
5	**74**	+1	33 ± 2	81 ± 3	44
6	**75**	+1	4.6 ± 0.2	83 ± 3	72
7	**76**	+1	-	-	-
8	**77**	+4	-	-	-
9	**78**	+4	0.86 ± 0.02	52 ± 2	59
10	**79**	+4	0.78 ± 0.09	70 ± 4	81
11	**80**	+4	1.0 ± 0.01	90 ± 4	100
12	**81**	+6	-	-	-
13	**82**	+4	6.1 ± 0.7	34 ± 3	28
14	**5a**	+4	1.5 ± 0.1	57 ± 3	60
15	**5b**	+4	1.3 ± 0.1	90 ± 5	96
16	**5c**	+4	1.4 ± 0.1	85 ± 5	90
17	**14b**	+2	190 ± 12	81 ± 3	22

[a]From DPX/HPTS export from EYPC-LUVs⊃DPX/HPTS at constant concentration of calf thymus DNA (1.25 μg/mL, ~4 μM phosphate), 10 mM Tris, 107 mM NaCl, pH 7.4, 25 °C, see **Fig. 5.6** and **5.13** (see **Experimental**), **70**, **71**, **76**, **77** and **81** were inactive (Y_{MAX} < 15%). [b]Maximal charge corresponding to the number of guanidinium/ammonium cations, ignoring possible charge reduction by proximity effects. [c]Effective activator concentration needed to reach 50% activity ($Y_{MAX/2}$), data ± SE. From Hill analysis of dose response curves (e.g., **Fig. 5.6**). [d]Maximal fractional fluorescence emission at saturation with activator relative to **72**, calculated after calibration to constant values after lysis. [e]Relative activator efficiency $\eta = f \times Y_{MAX} \times pEC_{50}$(mM), $f = 0.37$.

Countercations with alkyl tails (**70**-**75**) were better than aryl tails (**76**, **14b**). This trend was contrary to the charge-reversed situation with CPPs, where the high efficiency of aromatic counteranion activators was explained with their favorable partition into and translocation across bilayer membranes.[2,20] The reversed preference for alkyl over aryl activators with DNA carriers could suggest that activators **76** and **14b** preferably intercalate into the DNA duplex and thus prevent their aromatic tails to mediate partitioning into the bilayer membrane. However, poor efficiencies with polyions other than double-stranded DNA[3] did not support this interpretation (not shown).

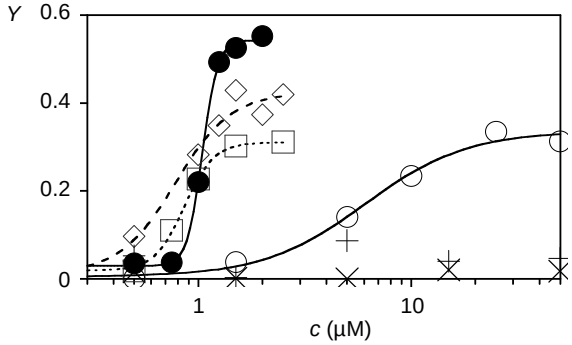

Fig. 5.6. Dose response curves for the activation of calf thymus DNA (1.25 μg/mL) by calixarenes **77** (x), **78** (□), **79** (◊), **80** (●), **81** (+) and **82** (○) in EYPC-LUV⊃HPTS/DPX.

Intercalation into DNA can be excluded with non-planar aromatic macrocycles such as calixarenes.[16] However, tetraguanidinium calix[4]arenes with insufficient amphiphilicity such as **77** failed to activate DNA transporters. Expansion to calix[6]arenes (**81**) did not solve the problem. Increasing amphiphilicity of calix[4]arenes resulted in increasing efficiency to activate DNA transporters. Considering the presence of four guanidinium cations per activator, the efficiency of calixarenes **78**-**80** and **5a-c** was comparable to or slightly better than that of the best alkylguanidinium activator **75**. However, comparisons at high activator efficiency should be done with caution because the beginning of stoichiometric binding can obscure significant differences.[21]

The bola-amphiphilic 1,3-alt isomer **72** was clearly less active and caused only 34% fluorescence recovery compared to the 52% of its amphiphilic isomer **78** (**Fig. 5.6**, ● vs ○). This important difference further supported amphiphilicity as essential characteristic of counterion activators. The acyclic analog **76** was >100-times less efficient than calix[4]arene **5b**. Multivalency, macrocyclic preorganization and competing intercalation into DNA probably contribute to this quite important calixarene effect.

5.2.4 DNA as Sensors in Lipid Bilayer Membranes

The discovery that CPP-counteranion complexes function as anion carriers in bulk and bilayer membranes was useful for the development of new drug delivery[4] and sensing systems.[8] The here reported discovery of the charge-inverted DNA-countercation complexes as cation carriers could therefore be expected to have a similarly diverse and important impact. Whereas cellular uptake of DNA-countercation complexes is extensively studied and routinely used in many variations,[15,16] their potential to function as multienzyme detectors and multianalyte sensors[10,11] remained to be clarified.

Among several possibilities to develop counterion-activated DNA transporters into sensing systems, inactivation by hydrophilic and anionic analytes was explored first. Phytate (or IP6) was selected as important representative of this family.[22] Competitive pairing of phytate with calixarene activator **5a** cleanly inactivated DNA transporters (**Fig. 5.7A**, ●, IC50 = 450 ± 30 nM). Similar inactivation did not occur with the completely dephosphorylated inositol (**Fig. 5.7A**, ○). Enzymatic phytate hydrolysis by incubation with phytase was detectable as fluorescence recovery caused by the activation of DNA-calixarene complexes (**Fig. 5.14**, see **Experimental**). This successful example for the detectability of enzyme activity with DNA-calixarene complexes implied that other approaches developed for synthetic pores[23] and CPP-counterion complexes[7,8] will be applicable to DNA-counterion complexes as well.

The applicability of DNA-calixarene complexes to sensing in complex matrices was then explored. Almond extracts were prepared following routine procedures.[22] DNA-counterion complexes were efficiently inactivated by these almond extracts (**Fig. 5.7B**, ●). Incubation of almond extracts with phytase practically removed their ability to inactivate DNA-counterion complexes (**Fig. 5.7B**, ○). This demonstrated that the inhibitory activity of almond extract originated mainly from phytate. Comparison of the IC50's before and after incubation with phytase with calibration curves afforded the expected phytate content (21 mg/g expected,[22] 25 ± 1 mg/g found).

The sensing of phytate and the related IP_7 has been explored previously with synthetic pores and CPP-counteranion complexes.[22] With CPP-counteranion complexes, phytate competes with the counteranion activator for binding to the polycation. With the complementary DNA-countercation complexes, phytate competes with the polyanion for binding to the countercation activator. Interestingly, phytate sensing revealed to be more sensitive with DNA (IC50 = 450 ± 30 nM) than with CPP transporters (IC50 = 5.4 ± 1.1 μM). However, counterion exchange in both sensing systems is less efficient than phytate binding within synthetic pores (IC50 = 45 ± 5 nM). Successful phytate sensing implied that related sensing approaches will be applicable to DNA-counterion complexes as well,[23] including the recent method to sense hydrophobic analytes with CPP-counterion complexes.[8] However, the most important sensing applications of stimuli-responsive DNA-counterion transporters will take advantage from DNA chemistry in the broadest sense, including the use of aptamers,[11] enzymes, intercalators, or more complex topologies.

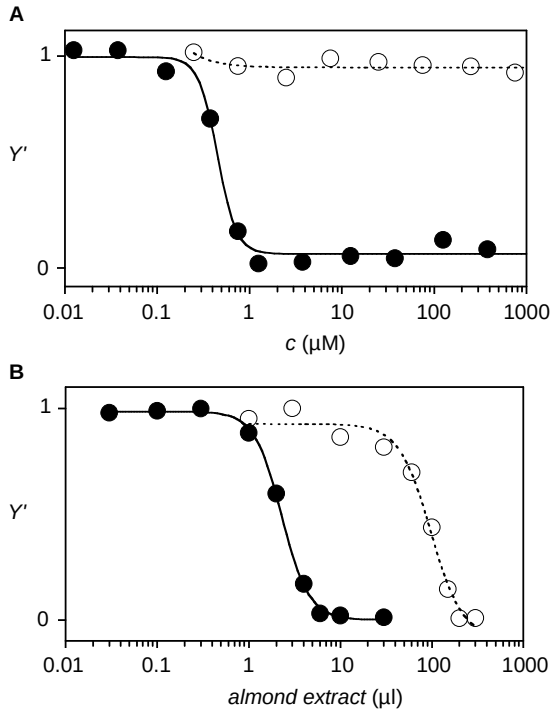

Fig. 5.7. Dose response curves for the inactivation of calf thymus DNA (1.25 μg/ml) and calixarene **5a** (2.5 μM) in EYPC-LUV⊃HPTS/DPX by (A) phytate (●) and inositol (○) and (B) almond extract before (●) and after phytase treatment (○). Fractional activities Y' are as in **Fig. 5.4**.

5.3 Conclusions

In summary, we provided compelling experimental evidence that amphiphilic counterions in complex with DNA can act as cation carriers, and showed that the active complexes can be used as detectors of enzyme activity and as multianalyte sensors in complex matrices. These results are important from a conceptual point of view[2,3] because counteranions have been shown previously to activate polycationic CPPs[1] not only for purposes of cellular uptake[4] but also as anion carriers,[2] multienzyme detectors[7] and multianalyte sensors.[8] The theoretical basis of counteranion-mediated multifunctionality has been clarified.[2,3] Complementary to the weak acidity of CPPs, DNA molecules are weakly basic polyanions. The evidence provided herein that DNA-counterion complexes can function as cation carriers, multienzyme detectors and multianalyte sensors is important because it demonstrates that the multifunctionality of polyion-counterion complexes is general, occurring with low-basicity polyanions exactly as with low-acidity polycations.

Stimulus-responsive DNA transporters, detectors, and sensors are of general and practical interest. Application of the lessons learned with CPP sensors concerning hydrophobic analytes, signal amplification, etc., will be straightforward and useful.[8,23] The prospective use of DNA for multianalyte sensing in fluorogenic,[13] chromogenic,[24] or chirogenic[25] vesicles is

particularly attractive. Current efforts focus on the use of DNA aptamers[11] as analyte-responsive transporters in membrane-based sensing systems. Considering the broader impact of research on counterion-activated CPPs,[1-8] research on counterion-activated DNA as transporters, detectors and sensors in vesicles is likely to influence other topics such as the development of non-viral gene vectors.

5.4 Experimental section

Materials

All salts and buffers were of the best grade available from Sigma or Fluka and used as received. 5(6)-carboxyfluorescein (CF) was from Fluka, 8-hydroxypyrene-1,3,6-trisulfonic acid trisodium salt (HPTS), safranin O and poly-L-lysine were from Sigma, and *p*-xylene-bis-pyridinium bromide (DPX) was from Invitrogen. Egg yolk phosphatidylcholine (EYPC), egg yolk phosphatidylglycerol (EYPG), dipalmitoylphosphatidylcholine (DPPC), and a Mini-Extruder used for vesicle preparation were from Avanti Polar Lipids. ESI-MS were performed on a Finnigan MAT SSQ 7000 instrument. ^{1}H and ^{13}C spectra were recorded on a Bruker 400 MHz spectrometer and are reported as chemical shifts (δ) in ppm relative to solvent peak. Spin multiplicities are reported as a singlet (s), doublet (d), triplet (t), with coupling constants (*J*) given in Hz, or multiplet (m). Fluorescence measurements were performed with a FluoroMax-2 spectrofluorometer (Jobin-Yvon Spex) equipped with a stirrer and a temperature controller. HPLC was performed using an Agilent 1100 series apparatus with a photodiode array detector. The U-tube experiments were performed using house made "U-tube". They consist of a small beaker (inner diameter, 16 mm) with a wall in the middle, separating two areas named *cis* and *trans* for the sampling and receiving areas, respectively. The $CHCl_3$ layers below the *cis* and *trans* aqueous phases are connected by a small opening (height, 6 mm) at the bottom of the wall separating the *cis* and *trans* buffers.

Abbreviations

CF: 5(6)-carboxyfluorescein; DMSO: dimethylsulfoxide; DPPC: dipalmitoylphosphatidylcholine; DPX: *p*-xylene-bispyridinium bromide; EYPC: egg yolk phosphatidylcholine; EYPG: egg yolk phosphatidylglycerol; HPTS: 8-hydroxypyrene-1,3,6-trisulfonic acid trisodium salt; LUVs: large unilamellar vesicles; Tris: tris(hydroxymethyl)aminomethane.

Synthesis of 1-dodecylguanidinium, chloride (74).

To a solution of 1-dodecylamine (1.4 g, 7.6 mmol) in EtOH (10 mL) was added 1H-Pyrazole-1-carboxamidine hydrochloride (1.2 g, 8.0 mmol). The reaction mixture was refluxed at 86 ˚C and stirred for 2.5 h. After stirring, the solvent was removed *in vacuo* and the crude product was recrystallized from EtOAc/petroleum ether (1:9) to give a pure guanidine as a white solid (1.5 g, 88%). ^{1}H NMR (400 MHz, $CDCl_3$/MeOD 19:1) δ 3.06 (t, *J* = 7.4 Hz, 2H, C*H*$_2$NH), 1.56-1.48 (m, 2H, C*H*$_2$CH$_2$NH), 1.32-1.14 (m, 18H, (C*H*$_2$)$_7$CH$_2$CH$_2$NH), 0.81 (t, *J* = 6.4 Hz, 3H, C*H*$_3$). ^{13}C NMR (100 MHz, $CDCl_3$/MeOD 19:1) δ 157.1, 41.6, 31.9, 29.6, 29.5, 29.4, 29.3, 28.7, 26.7, 22.7, 14.1. MS (ESI): calculated for $[M + H]^+$ *m*/*z* = 228.4, found *m*/*z* = 228.0.

Synthesis of 1-hexadecylguanidinium, chloride (75).

To a solution of 1-hexadecylamine (480 mg, 2.0 mmol) in EtOH (5 mL) was added 1H-Pyrazole-1-carboxamidine hydrochloride (308 mg, 2.1 mmol). The reaction mixture was refluxed at 86 ˚C and stirred for 2.5 h. After stirring, the solvent was removed *in vacuo* and the crude product was recrystallized from EtOAc/petroleum ether (1:9) to give a pure guanidine as a white solid (550 mg, 97%). ^{1}H NMR (400 MHz, $CDCl_3$/MeOD 19/1). δ 3.06 (t, *J* = 7.0 Hz, 2H, C*H*$_2$NH), 1.57-1.49 (m, 2H, C*H*$_2$CH$_2$NH), 1.31-1.16 (m, 26H, (C*H*$_2$)$_{11}$CH$_2$CH$_2$NH), 0.81 (t, *J* = 6.4 Hz, 3H, C*H*$_3$). ^{13}C NMR (400 MHz, $CDCl_3$/MeOD 19/1) δ 157.0, 41.6, 31.9, 29.7, 29.6, 29.4, 29.3, 28.7, 26.7, 22.7, 14.1. MS (ESI): calculated for $[M + H]^+$ *m*/*z* = 284.5, found *m*/*z* = 284.0.

Synthesis of Activators 77-82, **5a-5c** and **14b**.

Activators **77-82**, **5a-5c** and **14b** were prepared following previously reported procedures.[16]

U-Tube Experiments (Fig. 5.1)

$CHCl_3$ (3 mL) was placed in a U-tube and the *cis* and *trans* buffers were added on top of the organic layer: *cis* phase, aqueous buffer (10 mM Tris, 107 mM NaCl, pH 7.4) including calf thymus DNA (1.25 μg/mL), activator **74** (50 μM) and fluorescent dye(s); *trans* phase, aqueous buffer (10 mM Tris, 107 mM NaCl, pH 7.4). The organic layer was slowly stirred at room temperature. Aliquots were taken from the *trans* phase as a function of time. The concentration of safranin O (λ_{ex}, 519 nm; λ_{em}, 579 nm), CF (λ_{ex}, 490 nm; λ_{em}, 512 nm) and HPTS (λ_{ex}, 413 nm; λ_{em}, 508 nm) were determined from the fluorescence emission intensity of the diluted aliquots in comparison with the calibration curve. The concentration of DPX were determined by injecting those aliquots into the RP-HPLC instrument (column, YMC ProC8, 4 × 50 mm; mobile phase, linear gradient of 1% aqueous TFA to TFA/CH_3CN = 1/99

over 10 min; flow rate, 1 mL/min; UV detection at 260 nm, t_R = 0.81 min, solvent front: t_R = 0.57 min) and comparing the integration value with the calibration curve (**Fig. 5.1**).

General Procedures for Vesicle Experiments

i. Vesicle Preparation

A thin lipid film was prepared by evaporating a solution of 25 mg EYPC in 1 mL MeOH/$CHCl_3$ (1:1) on a rotary evaporator (r.t.) and then *in vacuo* overnight. The resulting film was hydrated with 1.0 mL buffer [5 mM HPTS, 16.5 mM DPX, 10 mM Tris, 72 mM NaCl, pH 7.4 (for EYPC-LUVs⊃HPTS/DPX, vesicle A) or 1 mM HPTS, 3.3 mM DPX, 10 mM Tris, 100 mM NaCl, pH 7.4 (for EYPC-LUVs⊃HPTS/DPX, vesicle B] for more than 30 min, subjected to freeze-thaw cycles (5×) and extrusions (15×) through a polycarbonate membrane (pore size, 100 nm). Extravesicular components were removed by gel filtration (Sephadex G-50) with 10 mM Tris, 107 mM NaCl, pH 7.4. Final conditions: ~5 mM EYPC; inside: 5 mM HPTS, 16.5 mM DPX, 10 mM Tris, 72 mM NaCl, pH 7.4 (for vesicle A) or 1 mM HPTS, 3.3 mM DPX, 10 mM Tris, 100 mM NaCl, pH 7.4 (for vesicle B); outside: 10 mM Tris, 107 mM NaCl, pH 7.4.

ii. Polyanion Activation Experiments

EYPC-LUV stock solutions were diluted with a buffer (10 mM Tris, 107 mM NaCl, pH 7.4) and placed in a thermostated fluorescence cuvette (25 ˚C) and gently stirred (total volume in the cuvette, ~2000 μL). HPTS efflux was monitored at λ_{em} 511 nm (λ_{ex} 413 nm) as a function of time after addition of cationic activators at t = 0 s (10 μL stock solution in DMSO), transporters at t = 50 s (20 μL stock solution in buffer) and 1.2% aqueous triton X-100 at t = 300 s (40 μL, 0.024% final concentration). Data were normalized to fractional emission intensity I(t) using equation (1)

$$I(t) = (I_t - I_0) / (I_\infty - I_0) \qquad (1)$$

where $I_0 = I_t$ at transporter addition, $I_\infty = I_t$ at saturation after lysis (e.g., **Fig. 5.8A**). Effective concentration EC_{50} and Hill coefficient n were determined by plotting the fractional activity Y (= I(t) at saturation before lysis, ~200 s) as a function of cationic activator concentration c_{cation} (or transporter concentration c_{DNA}) and fitting them to the Hill equation (2)

$$Y = Y_0 + (Y_{MAX} - Y_0) / \{1 + (EC_{50} / c_{cation})^n\} \qquad (2)$$

where Y_0 is Y without an cation (or DNA transporter), Y_{MAX} is a value with an excess cation (or DNA transporter) at saturation (e.g., **Fig. 5.8B**).

Poly(Lys)-Loaded Vesicles (Fig. 5.2 and 5.3)

i. Vesicle Preparation

A thin lipid film was prepared by evaporating a solution of 25 mg EYPC in 1 mL MeOH/$CHCl_3$ (1:1) on a rotary evaporator (r.t.) and then *in vacuo* overnight. The resulting film was hydrated with 1.0 mL buffer containing a varying concentration of poly(Lys) (5 mM HPTS, 16.5 mM DPX, 10 mM Tris, 0-100 μM poly(Lys), pH 7.4) for more than 30 min, subjected to freeze-thaw cycles (5×) and extrusions (15×) through a polycarbonate membrane (pore size, 100 nm). Extravesicular components were removed by gel filtration (Sephadex G-50) with 10 mM Tris, 107 mM NaCl, pH 7.4. Final conditions: ~5 mM EYPC; inside: 5 mM HPTS, 16.5 mM DPX, 0-100 μM poly(Lys), 10 mM Tris, 72 mM NaCl, pH 7.4.

ii. Polyanion Activation Experiments

The poly(Lys)-loaded EYPC-LUVs⊃HPTS/DPX stock solutions were diluted with buffer (10 mM Tris, 107 mM NaCl, pH 7.4) (~12.5 μM final EYPC concentration) and placed in a thermostated fluorescence cuvette (25 ˚C) and gently stirred. HPTS efflux was monitored at λ_{em} 511 nm (λ_{ex} 413 nm) as a function of time during addition of cationic activator **74** (50 μM), a varying concentration of calf thymus DNA (0-2.0 μg/mL final concentration) and 1.2% aqueous triton X-100 (0.024% final concentration). Data were normalized to fractional emission intensity *I* according to equation (1) (e.g., **Fig. 5.2A**), and EC_{50} and Hill coefficient *n* were determined by plotting the fractional activity *Y* (= *I* just before lysis, ~200 s) as a function of DNA transporter concentration c_{DNA} and fitting them to the Hill equation (2) (**Fig. 5.2B and Table 5.1**).

iii. DNA-Trapping Experiments with Poly(Lys)-Loaded Vesicles

The poly(Lys)-loaded EYPC-LUVs⊃HPTS/DPX (10 μM poly(Lys) inside) stock solutions were diluted with buffer (10 mM Tris, 107 mM NaCl, pH 7.4) (~12.5 μM final EYPC concentration) and placed in a thermostated fluorescence cuvette (25 ˚C) and gently stirred. HPTS efflux was monitored at λ_{em} 511 nm (λ_{ex} 413 nm) as a function of time during addition of cationic activator **74** (50 μM), calf thymus DNA (1 μg/mL at once, or 0.5 μg/ml first and then 0.125 μg/ml (4×) at every 150 s) and 1.2% aqueous triton X-100 (0.024% final concentration) (**Fig. 5.3A**). In either case, the final concentration of the DNA transporter in the cuvette is the same (1 μg/ml). The control experiments were performed with vesicles without poly(Lys) (**Fig. 5.3B**) and vesicles with external poly(Lys) (10 nM) (**Fig. 5.3C**).

HPTS/DPX Assay vs CF Assay (Fig. 5.4)

i. Vesicle Preparation for CF-Loaded Vesicles

A thin lipid film was prepared by evaporating a solution of 25 mg EYPC in 1 mL MeOH/$CHCl_3$ (1:1) on a rotary evaporator (r.t.) and then *in vacuo* overnight. The resulting

film was hydrated with 1.0 mL buffer (50 mM CF, 10 mM Tris, 10 mM NaCl, pH 7.4) for more than 30 min, subjected to freeze-thaw cycles (5×) and extrusions (15×) through a polycarbonate membrane (pore size, 100 nm). Extravesicular components were removed by gel filtration (Sephadex G-50) with 10 mM Tris, 107 mM NaCl, pH 7.4. Final conditions: ~5 mM EYPC; inside: 50 mM CF, 10 mM Tris, 10 mM NaCl, pH 7.4; outside: 10 mM Tris, 107 mM NaCl, pH 7.4.

ii. Polyanion Activation Experiments

The above EYPC-LUVs⊃CF or EYPC-LUVs⊃HPTS/DPX stock solutions were diluted with buffer (10 mM Tris, 107 mM NaCl, pH 7.4) (~75, ~50 and ~25 μM final EYPC concentration) and placed in a thermostated fluorescence cuvette (25 ˚C) and gently stirred. The fluorescent change was monitored at λ_{em} 517 nm (λ_{ex} 497 nm) for CF or at λ_{em} 511 nm (λ_{ex} 413 nm) for HPTS as a function of time during addition of a varying concentration of cationic activator **74**, calf thymus DNA (12.5 μg/mL final concentration) and 1.2% aqueous triton X-100 (0.024% final concentration). Data were normalized to fractional emission intensity *I* according to equation (1), and EC_{50} and Hill coefficient *n* were determined by plotting the fractional activity *Y* (= *I* just before lysis, ~200 s) as a function of canion concentration c_{cation} and fitting them to the Hill equation (2) (**Fig. 5.4**).

Dependence on Lipid Concentration

Varying volumes of EYPC-LUVs⊃HPTS/DPX stock solutions were diluted with buffer (10 mM Tris, 107 mM NaCl, pH 7.4) (total ~2 mL, ~6-190 μM final EYPC concentration) and placed in a thermostated fluorescence cuvette (25 ˚C) and gently stirred. HPTS efflux was monitored at λ_{em} 511 nm (λ_{ex} 413 nm) as a function of time during addition of activator **74** (50 μM, 75 μM or 100 μM final concentration), transporter (calf thymus DNA, poly(G) or oligonucleotide) and 1.2% aqueous triton X-100 (0.024% final concentration). Data were normalized to fractional emission intensity *I* according to equation (1), and EC_{50} and Hill coefficient *n* were determined by plotting the fractional activity *Y* (= *I* just before lysis, ~200 s) as a function of transporter concentration $c_{transporter}$ and fitting them to the Hill equation (2) (**Fig. 5.9**).

Dependence on Ionic Strength

i. Vesicle Preparation

A thin lipid film was prepared by evaporating a solution of 25 mg EYPC in 1 mL MeOH/$CHCl_3$ (1:1) on a rotary evaporator (r.t.) and then *in vacuo* overnight. The resulting film was hydrated with 1.0 mL buffer containing a varying concentration of NaCl (1 mM

HPTS, 3.3 mM DPX, 10 mM Tris, 0-1000 mM NaCl, pH 7.4) for more than 30 min, subjected to freeze-thaw cycles (5×) and extrusions (15×) through a polycarbonate membrane (pore size, 100 nm). Extravesicular components were removed by gel filtration (Sephadex G-50) with the extravesicular buffer containing a varying concentration of NaCl which is balanced with intravesicular ionic strength (10 mM Tris, 10-1000 mM NaCl, pH 7.4). Final conditions: ~5 mM EYPC; inside: 1 mM HPTS, 3.3 mM DPX, 10 mM Tris, 0-1000 mM NaCl, pH 7.4; outside: 10 mM Tris, 10-1000 mM NaCl, pH 7.4.

ii. Polyanion Activation Experiments

The above EYPC-LUVs⊃HPTS/DPX stock solutions were diluted with buffer containing the balanced salts (10 mM Tris, 10-1000 mM NaCl, pH 7.4) (~125 μM final EYPC concentration) and placed in a thermostated fluorescence cuvette (25 ˚C) and gently stirred. HPTS efflux was monitored at λ_{em} 511 nm (λ_{ex} 413 nm) as a function of time during addition of a varying concentration of cationic activator **74**, calf thymus DNA (12.5 μg/mL final concentration) and 1.2% aqueous triton X-100 (0.024% final concentration). Data were normalized to fractional emission intensity I according to equation (1), and EC_{50} and Hill coefficient n were determined by plotting the fractional activity Y (= I just before lysis, ~200 s) as a function of canion concentration c_{cation} and fitting them to the Hill equation (2) (**Fig. 5.10**).

Dependence on Membrane Fluidity

i. Preparation of DPPC-LUVs⊃HPTS/DPX

A thin lipid film was prepared by evaporating a solution of 25 mg DPPC in 1 mL MeOH/$CHCl_3$ (1:1) on a rotary evaporator (r.t.) and then *in vacuo* overnight. The resulting film was hydrated with 1.0 mL buffer (1 mM HPTS, 3.3 mM DPX, 10 mM Tris, 100 mM NaCl, pH 7.4) for more than 30 min at 60 ˚C (which is well above the phase transition temperature),[26] subjected to freeze-thaw cycles (5×, liquid N_2 and 60 ˚C water bath). The extruder was assembled and placed on top of a hot plate to warm up to 60 °C, which was controlled by measuring the temperature inside the extruder. The vesicle suspension was extruded (15×) through a polycarbonate membrane (pore size 100 nm) and extravesicular components were removed by gel filtration (Sephadex G-50) with 10 mM Tris, 107 mM NaCl, pH 7.4. Final conditions: ~5 mM EYPC; inside: 1 mM HPTS, 3.3 mM DPX, 10 mM Tris, 100 mM NaCl, pH 7.4; outside: 10 mM Tris, 107 mM NaCl, pH 7.4.

ii. Polyanion Activation Experiments

EYPC-LUVs⊃HPTS/DPX (vesicle b) or DPPC-LUVs⊃HPTS/DPX stock solutions were diluted with buffer (10 mM Tris, 107 mM NaCl, pH 7.4) (~125 μM final lipid concentration) and placed in a thermostated fluorescence cuvette (25-55 ˚C) and gently stirred. HPTS efflux was monitored at λ_{em} 511 nm (λ_{ex} 413 nm) as a function of time during addition of a varying concentration of cationic activator **74**, calf thymus DNA (12.5 μg/mL final concentration) and 1.2% aqueous triton X-100 (0.024% final concentration). Data were normalized to fractional emission intensity *I* according to equation (1), and EC_{50} and Hill coefficient *n* were determined by plotting the fractional activity *Y* (= *I* just before lysis, ~200 s) as a function of canion concentration c_{cation} and fitting them to the Hill equation (2) (**Fig. 5.11**).

Dependence on Negative Charge on Vesicle Surface

i. Vesicle Preparation

A thin lipid film was prepared by evaporating a solution of EYPC and EYPG (25 mg total) in 1 mL MeOH/$CHCl_3$ (1:1) on a rotary evaporator (r.t.) and then *in vacuo* overnight. The resulting film was hydrated with 1.0 mL buffer (5 mM HPTS, 16.5 mM DPX, 10 mM Tris, 72 mM NaCl, pH 7.4) for more than 30 min, subjected to freeze-thaw cycles (5×) and extrusions (15×) through a polycarbonate membrane (pore size, 100 nm). Extravesicular components were removed by gel filtration (Sephadex G-50) with 10 mM Tris, 107 mM NaCl, pH 7.4). Final conditions: ~5 mM lipid; inside: 5 mM HPTS, 16.5 mM DPX, 10 mM Tris, 72 mM NaCl, pH 7.4; outside: 10 mM Tris, 107 mM NaCl, pH 7.4.

ii. Polyanion Activation Experiments

EYPC/EYPG-LUVs⊃HPTS/DPX stock solutions were diluted with buffer (10 mM Tris, 107 mM NaCl, pH 7.4) (~12 μM final lipid concentration) and placed in a thermostated fluorescence cuvette (25 ˚C) and gently stirred. HPTS efflux was monitored at λ_{em} 511 nm (λ_{ex} 413 nm) as a function of time during addition of cationic activator **74** and calf thymus DNA (1.25 μg/mL final concentration) (for DNA activation), or dodecylphosphate and polyarginine (75 nM final concentration) (for pR activation), and 1.2% aqueous triton X-100 (0.024% final concentration). Data were normalized to fractional emission intensity *I* according to equation (1), and EC_{50} and Hill coefficient *n* were determined by plotting the fractional activity *Y* (= *I* just before lysis, ~200 s) as a function of activator concentration $c_{activator}$ and fitting them to the Hill equation (2) (**Fig. 5.12**).

Activator Screening (Fig. 5.6 and Table 5.2)

EYPC-LUVs⊃HPTS/DPX (vesicle A) stock solutions were diluted with buffer (10 mM Tris, 107 mM NaCl, pH 7.4) (~12 μM final EYPC concentration) and placed in a thermostated

fluorescence cuvette (25 ˚C) and gently stirred. HPTS efflux was monitored at λ_{em} 511 nm (λ_{ex} 413 nm) as a function of time during addition of all the cationic activators (15 nM-500 μM final concentration), calf thymus DNA (1.25 μg/mL final concentration) and 1.2% aqueous triton X-100 (0.024% final concentration). Data were normalized to fractional emission intensity *I* according to equation (1), and EC_{50} and Hill coefficient *n* were determined by plotting the fractional activity *Y* (= *I* just before lysis, ~200 s) as a function of canion concentration c_{cation} and fitting them to the Hill equation (2) (**Fig. 5.6** and **5.13**, **Table 5.2**).

Inhibition Experiments with Phytate (Fig. 5.7A)

EYPC-LUVs⊃HPTS/DPX stock solutions (vesicle A) were diluted with buffer (10 mM Tris, 107 mM NaCl, pH 7.4) and placed in a thermostated fluorescence cuvette (25 ˚C) and gently stirred. HPTS efflux was monitored at λ_{em} 511 nm (λ_{ex} 413 nm) as a function of time during addition of varying concentrations of phytate, activator **5a** (2.5 μM final concentration), calf thymus DNA (1.25 μg/mL final concentration) and 1.2% aqueous triton X-100 (0.024% final concentration). Data were normalized to fractional emission intensity *I* using equation (3)

$$I = (I_t - I_0) / (I_\infty - I_0) \quad (3)$$

where $I_0 = I_t$ at polyanion addition, $I_\infty = I_t$ at saturation after lysis. IC_{50} and Hill coefficient *n* were determined by plotting the fractional activity *Y* (= *I* just before lysis, ~200 s) as a function of phytate concentration $c_{phytate}$ and fitting them to the Hill equation (4)

$$Y = Y_\infty + (Y_0 - Y_\infty) / \{1 + (c_{phytate} / IC_{50})^n\} \quad (4)$$

where Y_0 is *Y* in the absence of phytate, Y_∞ is *Y* with excess phytate, IC_{50} is the concentration of phytate required for 50% inactivation and *n* is the Hill coefficient (**Fig. 5.7A**).

Detection of Phytase Activity

Phytate (500 μM) were incubated with phytase (0.03-1 units/mL) in 50 mM sodium acetate buffer, pH 5.5 at 58 °C. Aliquots (2.5 μL) were removed periodically and added to buffer (10 mM Tris, 107 mM NaCl, pH 7.4) containing EYPC-LUVs⊃HPTS/DPX (vesicle A) and activator **5a** (2.5 μM final concentration). Aliquots are to be diluted to a concentration of 1 μM in the cuvette. The time-dependent fluorescent change after addition of calf thymus DNA (1.25 μg/mL final concentration) was monitored, and activities, *Y*, were calculated and plotted as a function of time as described above (**Fig. 5.14**).

Phytate Sensing in Almonds (Fig. 5.7B)

i. Phytate Extraction Procedure.

The extraction procedure was modified from previously established methods.[27,28] 1 g of ground almonds were placed into a flask and defatted overnight by stirring in 30 mL petroleum ether. The sample was centrifuged, the supernatant was removed, and the solid precipitate was dried *in vacuo* for 1 h. The dried solid (0.413 g) was then extracted by stirring in 10 mL of 0.8 M HCl for 2 h. The sample was then centrifuged and the supernatant was collected. 3 mL of the supernatant was diluted with 50 mM sodium acetate buffer and adjusted pH with NaOH to 5.5 (total volume was adjusted to 15 mL).

ii. Inhibition Experiments with Almond Extract.

500 μL of the crude almond extract was diluted with 500 μL of 50 mM sodium acetate buffer (pH 5.5) and used for phytate sensing experiments. EYPC-LUVs⊃HPTS/DPX stock solutions (vesicle A) were diluted with buffer (10 mM Tris, 107 mM NaCl, pH 7.4) and placed in a thermostated fluorescence cuvette (25 ˚C) and gently stirred. HPTS efflux was monitored at λ_{em} 511 nm (λ_{ex} 413 nm) as a function of time during addition of varying volumes of the above almond extract (0-30 μL), activator **5a** (2.5 μM final concentration), calf thymus DNA (1.25 μg/mL final concentration) and 1.2% aqueous triton X-100 (0.024% final concentration). Fluorescence intensities were normalized as described above, and activities, *Y*, just before membrane lysis, were plotted as a function of extract volume. The resulting plot was fit to the Hill equation to obtain a V_{50} value, which is the volume of extract required for 50% inhibition, of 2.3 ± 0.07 μL (**Fig. 5.7B**).

iii. Inhibition Experiments with Phytase-Treated Almond Extract.

500 μL of the crude almond extract was added to 500 μL of buffer (50 mM sodium acetate, pH 5.5) containing 2 units/mL phytase, giving a final phytase concentration of 1 unit/mL. The solution was incubated at 58 °C for 1 h and used for inhibition experiments. EYPC-LUVs⊃HPTS/DPX stock solutions (vesicle A) were diluted with buffer (10 mM Tris, 107 mM NaCl, pH 7.4) and placed in a thermostated fluorescence cuvette (25 ˚C) and gently stirred. HPTS efflux was monitored at λ_{em} 511 nm (λ_{ex} 413 nm) as a function of time during addition of varying volumes of the digested almond extract (0-300 μL), activator **5a** (2.5 μM final concentration), calf thymus DNA (1.25 μg/mL final concentration) and 1.2% aqueous triton X-100 (0.024% final concentration). Fluorescence intensities were normalized as described above, and activities, *Y*, just before membrane lysis, were plot as a function of extract volume. The resulting plot was fit to the Hill equation to obtain a V_{50} value, which is the volume of extract required for 50% inhibition for the digested extract, of 97 ± 12 μL (**Fig. 5.7B**).

iv. Determination of Phytate Content in Almonds.

The inhibition with the phytase-treated almond extract results from unknown inhibitors in the extract which are not phytate, as all of the phytate has been consumed after enzymatic treatment. Upon fitting the dose-response curves to the Hill equation, a V_{50} of 2.3 ± 0.07 μL was obtained for the almond extract and a V_{50} of 97 ± 12 μL was obtained for the phytase-treated extract. With the assumption that the inhibition in the undigested extract results from phytate inhibition, the addition of 2.3 (± 0.07) μL almond extract to the cuvette leads to a concentration equal to the IC_{50} of phytate determined from calibration curves (**Fig. 5.7A**, IC_{50} = 450 ± 30 nM). By multiplying this concentration by the dilution factor in the cuvette, we obtain an estimate for the phytate concentration in the almond extract. Because this estimated phytate concentration erroneously includes other inhibitors than phytate in the crude extract, contributions from non-phytate inhibitors has to be excluded by subtracting the result of the enzyme-treated extract from the above estimated phytate value. Specifically, the phytate concentration in the almond extract, *c*, was determined by equation (5),

$$c = (IC_{50} \times V_{tot} / V_{50}) - (IC_{50} \times V_{tot} / V_{50,phytase}) \quad (5)$$

where V_{50} is the volume of the almond extract (not treated with phytase) required for 50% inhibition (2.3 ± 0.07 μL), $V_{50,phytase}$ is the volume for the phytase-treated extract required for 50% inhibition (97 ± 12 μL), IC_{50} is the phytate concentration required for 50% inhibition which is determined from the calibration curve of a phyate sample of known concentration (450 ± 30 nM), and V_{tot} is the total volume in the fluorescence cuvette (2010 μL). By applying this equation to the almond extract used for phytate sensing experiments, we obtained a phytate concentration of 384 ± 21 μM. In order to translate this value into a concentration of phytate in the almond, the concentration of almond extract was converted to the mass of phytate extracted, $M_{phytate}$, according to equation (6),

$$M_{phytate} = c\ (\mu M) \times 0.010\ (L) \times 10 \times 660\ (g/mol) \quad (6)$$

where 0.010 (L) is the total volume of 0.8 M HCl used for extracting phytate from the almond powder, 660 g/mol is the MW of phytate, and multiplication by 10 accounts for the fact that the HCl supernatant after centrifugation was diluted 5 times with buffer, and further diluted (×2) with buffer just before vesicle experiments in both cases. By this analysis, we obtain a $M_{phytate}$ value of 25.3 ± 1.4 mg. $M_{phytate}$ was then divided by the total mass of almond sample used, M_{sample} (1 g), by equation (7)

$$PC_{sample} = M_{phytate}/M_{sample} \quad (7)$$

to obtain the final phytate content, PC_{sample}, in the almond solid as 25 ± 1 mg/g. The error in the PC_{sample} value is determined from curve fitting errors. The PC_{sample} value is in agreement with the value of 21 mg/g and 19 ± 2 mg/g determined in the literature using an HPLC method[28] and synthetic pores[8] respectively.

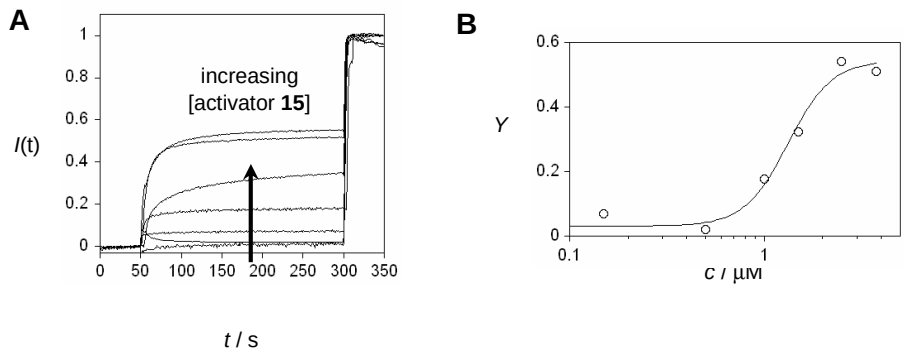

Fig. 5.8. (**A**) Representative normalized kinetics of transporter-mediated increase in HPTS fluorescence, following addition of calf thymus DNA (1.25 μg/mL final concentration) at t = 50 s and triton X-100 (0.024% final concentration) at t = 300 s, demonstrating increasing DNA transporter activity with increasing concentrations of activator **5a** (0.05-3.75 μM). (**B**) Representative dose-response curve for DNA activation with activator **5a** obtained by plotting the fractional activity Y against concentration of activator **5a**, giving EC_{50} for **5a** of 1.3 ± 0.1 μM and Y_{MAX} of 54 ± 4%.

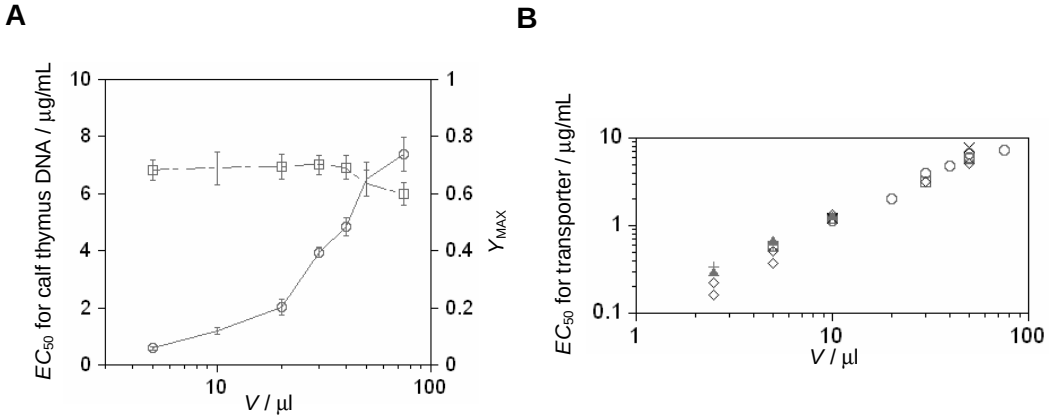

Fig. 5.9. Optimization of lipid concentration for transporter activation with activator **74**. (**A**) EC_{50} (○) and Y_{MAX} (□) for calf thymus DNA in the presence of activator **74** (100 μM) in EYPC-LUVs⊃HPTS/DPX were plotted as a function of vesicle volume V. (**B**) EC_{50} for calf thymus DNA (○, □, ◊), poly(G) (×, +) and 29-mer oligonucleotide (▲) in the presence of 50 μM (◊, +, ▲), 75 μM (□) and 100 μM (○, ×) activator **74** in EYPC-LUVs⊃HPTS/DPX were plotted as a function of vesicle volume V. 10 μL of vesicle volume corresponds to ~25 μM final EYPC concentration.

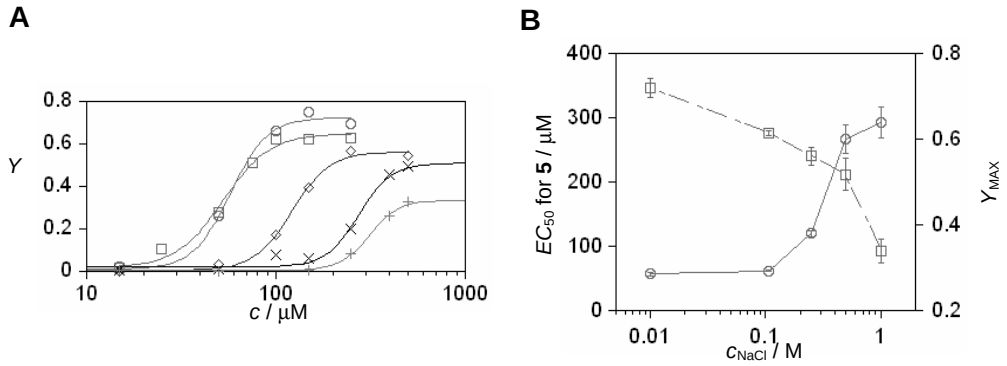

Fig. 5.10. Dependence of DNA activation with activator **74** on ionic strength. (**A**) Dose-response curves for the activation of calf thymus DNA (12.5 µg/mL final concentration) by activator **74** in the presence of 10 mM (○), 107 mM (□), 250 mM (◊), 500 mM (×) and 1000 mM (+) NaCl. (**B**) EC_{50} (○) and Y_{MAX} (□) for **74** were plotted as a function of NaCl concentration.

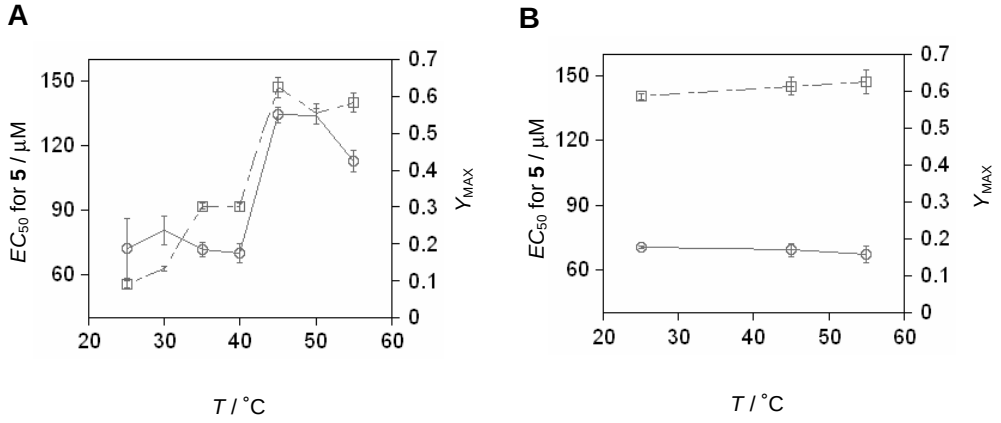

Fig. 5.11. Dependence of DNA activation with activator **74** on membrane fluidity. EC_{50} (○) and Y_{MAX} (□) for **74** in DPPC-LUVs⊃HPTS/DPX (**A**) and EYPC-LUVs⊃HPTS/DPX (**B**) were plotted as a function of temperature. The dotted line in **A** indicates the phase transition of DPPC at 41.4 ˚C.

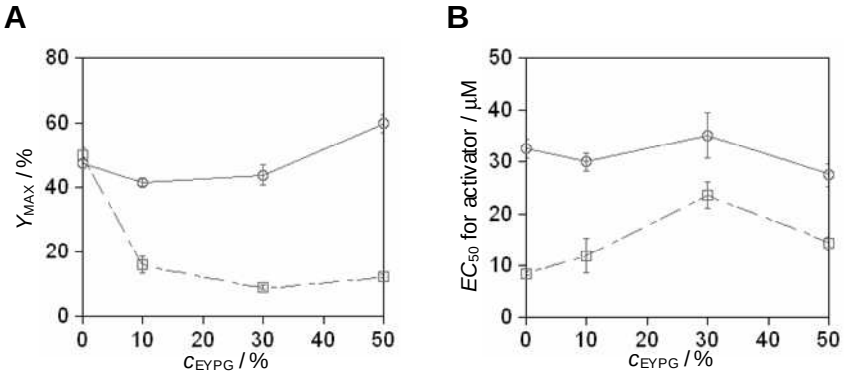

Fig. 5.12. Dependence of transporter activation with amphiphilic activator on surface negative charge on vesicle. Y_{MAX} (**A**) and EC_{50} (**B**) for calf thymus DNA/activator **74** (○) and polyarginine/dodecylphosphate (□) were plotted as a function of EYPG concentration in EYPC/EYPG-LUVs⊃HPTS/DPX.

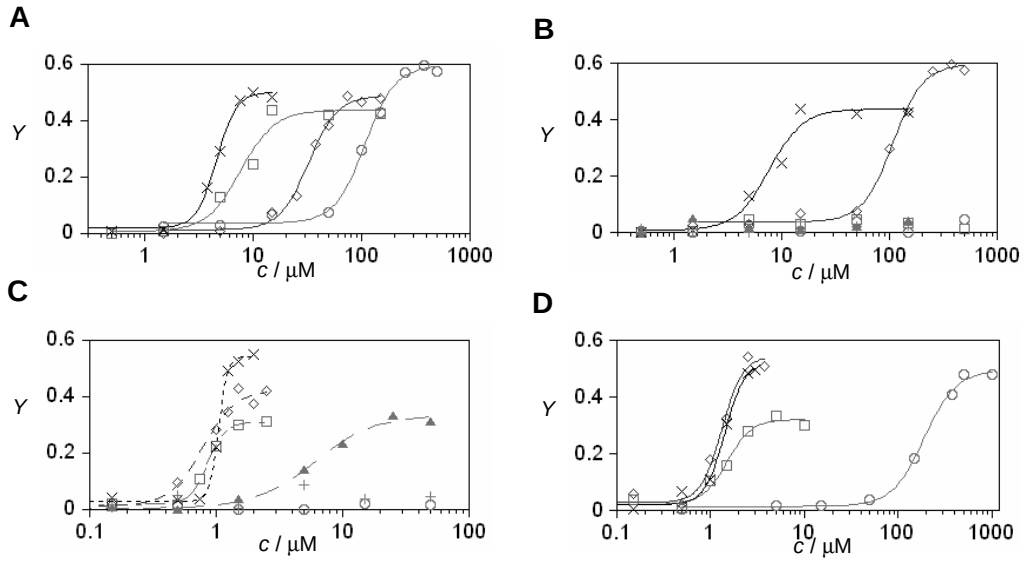

Fig. 5.13. Activator screening for DNA activation. (**A**-**D**) Dose-response curves for the activation of calf thymus DNA (1.25 μg/mL final concentration) by **70** (○ in **B**), **71** (□ in **B**), **72** (○ in **A**, ◊ in **B**), **73** (□ in **A**, × in **B**), **74** (◊ in **A**), **75** (× in **A**), **76** (▲ in **A**), **77** (○ in **C**), **78** (□ in **C**), **79** (◊ in **C**), **80** (× in **C**), **81** (+ in **C**), **82** (▲ in **C**), **5b** (□ in **D**), **5a** (◊ in **D**), **5c** (× in **D**), **14b** (○ in **D**).

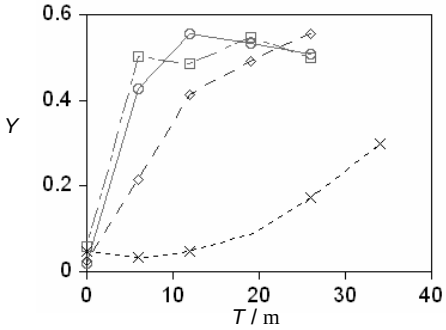

Fig. 5.14. Monitoring enzyme activity with DNA activation by activator **5a**. Phytase activity was detected with the activation of calf thymus DNA (1.25 μg/mL) by activator **5a** (2.5 μM) upon conversion of phytate (strong inhibitor) to inositol (inactive) with 1 (○), 0.3 (□), 0.1 (◊) and 0.03 (×) units/ml phytase. Fractional activity *Y* was plotted as a function of incubation time with phytase.

5.5 References

[§]The results reported in this chapter have been already published in Takeuchi, T.; Bagnacani, V.; Sansone, F.; Matile, S. *ChemBioChem* **2009**, *10*, 2793-2799.

1. a) Inomata, K.; Ohno, A.; Tochio, H.; Isogai, S.; Tenno, T.; Nakase, I.; Takeuchi, T.; Futaki, S.; Ito, Y.; Hiroaki, H.; Shirakawa, M. *Nature* **2009**, *458*, 106-109; b) Jablonski, A. E.; Humphries, W. H.; Payne, C. K. *J. Phys. Chem. B*, **2009**, *113*, 405-408; c) Nakase, I.; Takeuchi, T.; Tanaka, G.; Futaki, S. *Adv. Drug Del. Rev.* **2008**, *60*, 598-607; d) Wender, P. A.; Galliher, W. C.; Goun, E. A.; Jones, L. R.; Pillow, T. H. *Adv. Drug Del. Rev.* **2008**, *60*, 452-472; e) Ziegler, A. *Adv. Drug Del. Rev.* **2008**, *60*, 580-597; f) Smith, B. A.; Daniels, D.

S.; Coplin, A. E.; Jordan, G. E.; McGregor, L. M.; Schepartz, A. *J. Am. Chem. Soc.* **2008**, *130*, 2948-2949; g) Kolonko, E. M.; Kiessling, L. L. *J. Am. Chem. Soc.* **2008**, *130*, 5626-5627; h) Elson-Schwab, L.; Garner, O. B.; Schuksz, M.; Crawford, B. E.; Esko, J. D.; Tor, Y. *J. Biol. Chem.* **2007**, *282*, 13585-13591; i) Esbjorner, E. K.; Lincoln, P.; Norden, B. *Biochem. Biophys. Acta* **2007**, *1768*, 1550-1558; j) Fuchs, S. M.; Raines, R. T. *ACS Chem. Biol.* **2007**, *2*, 167-170; k) Shimanouchi, T.; Walde, P.; Gardiner, J.; Mahajan, Y. R.; Seebach, D.; Thomae, A.; Kraemer, S. D.; Voser, M.; Kuboi, R. *Biochem. Biophys. Acta* **2007**, *1768*, 2726-2736; l) Tang, M.; Waring, A. J.; Hong, M. *J. Am. Chem. Soc.* **2007**, *129*, 11438-11446; m) Gump, J. M.; Dowdy, S. F. *Trends Mol. Med.* **2007**, *13*, 443-448; n) Holowka, E. P.; Sun, V. Z.; Kamei, D. T.; Deming, T. J. *Nat. Mater.* **2007**, *6*, 52-57; o) Goun, E. A.; Pillow, T. H.; Jones, L. R.; Rothbard, J. B.; Wender, P. A. *ChemBioChem* **2006**, *7*, 1497-1515; p) Pujals, S.; Fernandez-Carneado, J.; Lopez-Iglesias, C.; Kogan, M. J.; Giralt, E. *Biochem. Biophys. Acta* **2006**, *1758*, 264-279; q) Tsogas, I.; Tsiourvas, D.; Nounesis, G.; Paleos, C. M. *Langmuir* **2006**, *22*, 11322-11328; r) Wolf, Y.; Pritz, S.; Abes, S.; Bienert, M.; Lebleu, B.; Oehlke, J. *Biochemistry* **2006**, *45*, 14944-14954; s) Afonin, S.; Frey, A.; Bayerl, S.; Fischer, D.; Wadhwani, P.; Weinkauf, S.; Ulrich, A. S. *ChemPhysChem* **2006**, *7*, 2134-2142; t) Barnay-Wallje, E.; Andersson, A.; Graslund, A.; Maler, L. J. *Biomol. NMR* **2006**, *35*, 137-147; u) Goncalves, E.; Kitas, E.; Seelig, J. *Biochemistry* **2005**, *44*, 2692-2702; v) Fischer, R.; Fotin-Mleczek, M.; Hufnagel, H.; Brock, R. *ChemBioChem* **2005**, *6*, 2126-2142; w) Jiang, T.; Olson, E. S.; Nguyen, Q. T.; Roy, M.; Jennings, P. A.; Tsien, R. Y. *Proc. Natl. Acad. Sci. USA* **2004**, *101*, 17867-17872; x) Futaki, S., Ed. *Curr. Protein Pept. Sci.* **2003**, *4*, 87-157; y) Brigati, C.; Giacca, M.; Noonan, D. M.; Albini, A. *FEMS Microbiol. Lett.* **2003**, *220*, 57-65; z) Ryser, H. J.; Hancock, R. *Science* **1965**, *150*, 501-503.

2. a) Sakai, N.; Matile, S. *J. Am. Chem. Soc.* **2003**, *125*, 14348-14356; b) Nishihara, M.; Perret, F.; Takeuchi, T.; Futaki, S.; Lazar, A. N.; Coleman, A. W.; Sakai, N.; Matile, S. *Org. Biomol. Chem.* **2005**, *3*, 1659-1669; c) Sakai, N.; Takeuchi, T.; Futaki, S.; Matile, S. *ChemBioChem* **2005**, *6*, 114-122.

3. a) Takeuchi, T.; Sakai, N.; Matile, S. *Faraday Trans., Faraday Discuss.* **2009**, *143*, 187-20; b) Sakai, N.; Futaki, S.; Matile, S. *Soft Matter* **2006**, *2*, 636-641.

4. Takeuchi, T.; Kosuge, M.; Tadokoro, A.; Sugiura, Y.; Nishi, M.; Kawata, M.; Sakai, N.; Matile, S.; Futaki, S. *ACS Chem. Biol.* **2006**, *1*, 299-303.

5. a) Schmidt, D.; Jiang, Q. X.; MacKinnon R. *Nature* **2006**, *444*, 775-779; b) Tieleman, D. P.; Robertson, K. M.; Maccallum, J. L.; Monticelli, L. *Int. J. Quantum Chem.* **2004**, *100*, 1071-1078.

6. Sakai, N.; Sordé, N.; Das, G.; Perrottet, P.; Gerard, D.; Matile, S. *Org. Biomol. Chem.* **2003**, *1*, 1226-1231.

7. Miyatake, T.; Nishihara, M.; Matile, S. *J. Am. Chem. Soc.* **2006**, *128*, 12420-12421.

8. Butterfield, S. M.; Miyatake, T.; Matile, S. *Angew. Chem. Int. Ed.* **2009**, *48*, 325-328.

9. a) Rebek, J. Jr.; Askew, B.; Nemeth, D.; Parris, K. *J. Am. Chem. Soc.* **1987**, *109*, 2432-2434; b) Breccia, P.; Van Gool, M.; Pérez-Fernández, R.; Martín-Santamaría, S.; Gago, F.; Prados, P.; de Mendoza, J. *J. Am. Chem. Soc.* **2003**, *125*, 8270-8284; c) Pérez-Fernández, R.; Pittelkow, M.; Belenguer, A. M.; Sanders, J. K. M. *Chem. Commun.* **2008**, 1738-1740.

10. a) Reymond, J.-L.; Fluxa, V. S.; Maillard, N. *Chem. Commun.* **2009**, 34-46; b) Wada, A.; Tamaru, S.; Ikeda, M.; Hamachi, I. *J. Am. Chem. Soc.* **2009**, *131*, 5321-5330; c) Vial, L.; Dumy, P. *New J. Chem.* **2009**, *33*, 939-946; d) Schrader, T.; Ed. Creative Chemical Sensing Systems. Topics in Current Chemistry, Springer, Heidelberg, **2007**; e) Hennig, A.; Bakirci, H.; Nau, W. M. *Nat. Methods* **2007**, *4*, 629-632; f) Palacios, M. A.; Nishiyabu, R.; Marquez, M.; Anzenbacher, P. *J. Am. Chem. Soc.* **2007**, *129*, 7538-7544; g) Buryak, A.; Pozdnoukhov, A.; Severin, K. *Chem. Commun.* **2007**, 2366-2368; h) Zhang, C.; Suslick, K. S. *J. Agric. Food Chem.* **2007**, *55*, 237-242; i) Wright, A. T.; Anslyn, E. V. *Chem. Soc. Rev.* **2006**, *35*, 14-28; j) Guarise, C.; Pasquato, L.; De Filippis, V.; Scrimin, P. *Proc. Natl. Acad. Sci. USA* **2006**, *103*, 3978-3982. (k) Nelson, T. L.; O'Sullivan, C.; Greene, N. T.; Maynor, M. S.; Lavigne, J. J. *J. Am. Chem. Soc.* **2006**, *128*, 5640-5641; l) Janzen, M. C.; Ponder, J. B.; Bailey, D. P.; Ingison, C. K.; Suslick, K. S. *Anal. Chem.* **2006**, *78*, 3591-3600; m) Rissin, D. M.; Walt, D. R. *J. Am. Chem. Soc.* **2006**, *128*, 6286-6287; n) Tamaru, S.; Kiyonaka, S.; Hamachi, I. *Chem. Eur. J.* **2005**, *11*, 7294-7304; o) Sanz Alaejos, M.; Garcìa Montelongo, F. *J. Chem. Rev.* **2004**, *104*, 3239-3265; p) Marquette, C. A.; Degiuli, A.; Blum, L. *J. Biosens. Bioelectron.* **2004**, *19*, 433-439; q) Campanella, L.; Bonanni, A.; Finotti, E.; Tomassetti, M. *Biosens. Bioelectron.* **2004**, *19*, 641-651; r) Goddard, J.-P.; Reymond, J.-L. *Curr. Opin. Biotechnol.* **2004**, *15*, 314-322; s) Houseman, B. T.; Huh, J. H.; Kron, S. J.; Mrksich, M. *Nat. Biotechnol.* **2002**, *20*, 270-274; t) Lavigne, J. J.; Anslyn, E. V. *Angew. Chem. Int. Ed.* **2001**, *40*, 3118-3130; u) Lavigne, J. J.; Anslyn, E. V. *Angew. Chem. Int. Ed.* **2001**, *40*, 3118-3130; v) Rakow, N. A.; Suslick, K. S. *Nature* **2000**, *406*, 710-703; w) Toko, K. *Biosens. Bioelectron.* **1998**, *13*, 701-709.

11. a) Li, M.; Lin, N.; Huang, Z.; Du, L.; Altier, C.; Fang, H.; Wang, B. *J. Am. Chem. Soc.* **2008**, *130*, 12636-12638; b) Willner, I.; Zayats, M. *Angew. Chem. Int. Ed.* **2007**, *46*, 6408-6418; c) Liu, J.; Lu, Y. *Angew. Chem. Int. Ed.* **2006**, *45*, 90-94.

12. Haugland, R. P. The Handbook. A Guide to Fluorescent Probes and Labeling Techniques, 10th edition, Invitrogen, **2005**.

13. Matile, S.; Sakai, N. The Characterization of Synthetic Ion Channels and Pores. In Analytical Methods in Supramolecular Chemistry, Schalley, C. A., Ed.; Wiley, Weinheim, **2007**, 391-418.

14. a) Mehiri, M.; Chen, W.-H.; Janout, V.; Regen, S. L. *J. Am. Chem. Soc.* **2009**, *131*, 1338-1339; b) Janout, V.; Jing, B.; Regen, S. L. *J. Am. Chem. Soc.* **2005**, *127*, 15862-15870; c) McNally, B. A.; Koulov, A. V.; Lambert, T. N.; Smith, B. D.; Joos, J. B.; Sisson, A. L.; Clare, J. P.; Sgarlata, V.; Judd, L. W.; Magro, G.; Davis, A. P. *Chem. Eur. J.* **2008**, *14*, 9599-9606; d) McNally, B. A.; Koulov, A. V.; Smith, B. D.; Joos, J. B.; Davis, A. P. *Chem. Commun.* **2005**, 1087-1089.

15. a) Srinivasachari, S.; Fichter, K. M.; Reineke, T. M. *J. Am. Chem. Soc.* **2008**, *130*, 4618 4627; b) Fletcher, S.; Ahmad, A.; Price, W. S.; Jorgensen, M. R.; Miller, A. D. *ChemBioChem* **2008**, *9*, 455-463; c) Tziveleka, L.-A.; Psarra, A.-M. G.; Tsiourvas, D.; Paleos, C. M. *J. Controlled Release* **2007**, *117*, 137-146; d) Guillot-Nieckowski, M.; Eisler, S.; Diederich, F. *New J. Chem.* **2007**, *31*, 1111-1127; e) Rajesh, M.; Sen, J.; Srujan, M.; Mukherjee, K.; Sreedhar, B.; Chaudhuri, A. *J. Am. Chem. Soc.* **2007**, *129*, 11408-11420; f) Wasungu, L.; Hoekstra, D. *J. Controlled Release* **2006**, *116*, 255-264; g) Li, H.-Y.; Birchall, *J. Pharm. Res.* **2006**, *23*, 941-950; h) Horiuchi, S.; Aoyama, Y. *J. Controlled Release* **2006**, *116*, 107-114; i) Kostarelos, K.; Miller, A. D. *Chem. Soc. Rev.* **2005**, *34*, 970-994; j) Sainlos, M.; Hauchecorne, M.; Oudrhiri, N.; Zertal-Zidani, S.; Aissaoui, A.; Vigneron, J.-P.; Lehn, J.-M.; Lehn, P. *ChemBioChem* **2005**, *6*, 1023-1033; k) Dass, C. R. *J. Mol. Med.* **2004**, *82*, 579-591; l) Zhanga, S.; Xu, Y.; Wang, B.; Qiao, W.; Liu, D.; Li, Z. *J. Controlled Release* **2004**, *100*, 165-180; m) Haag, R. *Angew. Chem. Int. Ed.* **2004**, *43*, 278-282; n) Kirby, A. J.; Camilleri, P.; Engberts, J. B. F. N.; Feiters, M. C.; Nolte, R. J. M.; Söderman, O.; Bergsma, M.; Bell, P. C.; Fielden, M. L.; García Rodríguez, C. L.; Guédat, P.; Kremer, A.; McGregor, C.; Perrin, C.; Ronsin, G.; van Eijk, M. C. P. *Angew. Chem. Int. Ed.* **2003**, *42*, 1448-1457; o) Aissaoui, A.; Oudrhiri, N.; Petit, L.; Hauchecorne, M.; Kan, E.; Sainlos, M.; Julia, S.; Navarro, J.; Vigneron, J.-P.; Lehn, J.-M.; Lehn, P. *Curr. Drug Targets* **2002**, *3*, 1-16; p) Zabner, J. *Adv. Drug. Delivery Rev.* **1997**, *27*, 17-28; q) Felgner, P. L.; Gadek, T. R.; Holm, M.; Roman, R.; Chan, H. W.; Wenz, M.; Northrop, J. P.; Ringold, G. M.; Danielsen, M. *Proc. Natl. Acad. Sci. USA* **1987**, *84*, 7413-7417.

16. a) Bagnacani, V.; Sansone, F.; Donofrio, G.; Baldini, L.; Casnati, A.; Ungaro, R. *Org. Lett.* **2008**, *10*, 3953-3956; b) Sansone, F.; Dudic, M.; Donofrio, G.; Rivetti, C.; Baldini, L.; Casnati, A.; Cellai, S.; Ungaro, R. *J. Am. Chem. Soc.* **2006**, *128*, 14528-14536.

17. Matile, S.; Som, A.; Sordé, N. *Tetrahedron* **2004**, *60*, 6405-6435.

18. a) Otto, S.; Osifchin, M.; Regen, S. L. *J. Am. Chem. Soc.* **1999**, *121*, 10440-10441; b) Koulov, A. V.; Lambert, T. N.; Shukla, R.; Jain, M.; Boon, J. M.; Smith, B. D.; Li, H.; Sheppard, D. N.; Joos, J. B.; Clare, J. P.; Davis, A. P. *Angew. Chem. Int. Ed.* **2003**, *42*, 4931-4933.

19. Blondeau, P.; Segura, M.; Pérez-Fernández, R.; de Mendoza, J. *Chem. Soc. Rev.* **2007**, *36*, 198-210; b) Schug, K. A.; Lindner, W. *Chem. Rev.* **2005**, *105*, 67-113; c) Best, M. D.; Tobey, S. L.; Anslyn, E. V. *Coord. Chem. Rev.* **2003**, *240*, 3-15.

20. a) Sanderson, J. M.; Whelan, E. *J. Phys. Chem. Chem. Phys.* **2004**, *6*, 1012-1017; b) Ridder, A. N. J. A.; Morein, S.; Stam, J. G.; Kuhn, A.; de Kruijff, B.; Killian, J. A. *Biochemistry* **2000**, *39*, 6521-6528; c) Yau, W. M.; Wimley, W. C.; Gawrisch, K.; White, S. H., *Biochemistry* **1998**, *37*, 14713-14718.

21. a) Mora, F.; Tran, D.-H.; Oudry, N.; Hopfgartner, G.; Jeannerat, D.; Sakai, N.; Matile, S. *Chem. Eur. J.* **2008**, *14*, 1947-1953; b) Soichet, B. K. *J. Med. Chem.* **2006**, *49*, 7274-7277; c) Straus, O. H.; Goldstein, A. *J. Gen. Physiol.* **1943**, *26*, 559-585.

22. Butterfield, S. M.; Tran, D.-H.; Zhang, H.; Prestwich, G. D.; Matile, S. *J. Am. Chem. Soc.* **2008**, *130*, 3270-3271.

23. a) Litvinchuk, S.; Tanaka, H.; Miyatake, T.; Pasini, D.; Tanaka, T.; Bollot, G.; Mareda, J.; Matile, S. *Nat. Mater.* **2007**, *6*, 576-580; b) Das, G.; Talukdar, P.; Matile, S. *Science* **2002**, *298*, 1600-1602.

24. Butterfield, S. M.; Hennig, A.; Matile S. *Org. Biomol. Chem.* **2009**, *7*, 1784-1792.

25. Hennig, A.; Matile, S. *Chirality* **2008**, *20*, 932-937.

26. Biltonen, R. L.; Lichtenberg, D. *Chem. Phys. Lipids* **1993**, *64*, 129-142.

27. Latta, M.; Eskin, M. J. *Agric. Food. Chem.* **1980**, *28*, 1313-1315.

28. Harlan, B. F.; Smikle-Williams, S.; Oberleas, D. *J. Food Comp. Anal*. **2004**, *17*, 227-233.